Published in final edited form as:
Eur J Inorg Chem. 2012 April ; 2012(12): 2099–2107. doi:10.1002/ejic.201101362.

Synthesis, Characterization, and in vitro Testing of a Bacteria-Targeted MR Contrast Agent

Lauren M. Matosziuk[a],[‡], **Allison S. Harney**[a],[‡], **Keith W. MacRenaris**[a], and **Thomas J. Meade**[a]

[a] Departments of Chemistry, Molecular Biosciences, Neurobiology, Biomedical Engineering, and Radiology, Northwestern University, 2145 Sheridan Rd., Evanston, IL 60208, USA

Abstract

A bacteria-targeted MR contrast agent, Zn-**1**, consisting of two Zn-dipicolylamine (Zn-dpa) groups conjugated to a Gd^{III} chelate has been synthesized and characterized. In vitro studies with *S. aureus* and *E. coli* show that Zn-**1** exhibits a significant improvement in bacteria labeling efficiency vs. control. Studies with a structural analogue, Zn-**2**, indicate that removal of one Zn-dpa moiety dramatically reduces the agent's affinity for bacteria. The ability of Zn-**1** to significantly reduce the T_1 of labeled vs. unlabeled bacteria, resulting in enhanced MR image contrast, demonstrates its potential for visualizing bacterial infections in vivo.

Keywords

Medicinal chemistry; Imaging agents; Magnetic resonance imaging; Bacteria labeling; Zinc

Introduction

With the advancement of medical treatments and technologies, bacterial infection has become a growing concern in the course of patient care.[1] In the United States, approximately 2 million hospital patients develop a hospital-acquired infection each year.[1] Due to illness, organ transplantation, or specific disease treatments, many patients possess a depressed immune system that renders the individual more susceptible to infection.[2] Further, prosthetic materials such as stents, mesh grafts, and catheters can provide additional microenvironments for bacterial growth.[3] Antibiotic-resistant bacteria strains increase the severity of illness, length of hospital stay and mortality from infection.[4] Consequently, new agents and techniques to prevent, diagnose, and treat bacterial infection are of interest.

Typically an accurate diagnosis of bacterial infection is derived from cultures of samples obtained from the site of suspected infection. Other clinical methods to identify infection include monitoring of body temperature, white blood cell count, erythrocyte sedimentation rate and cytokine reactions – none of which are a *specific* response to infection.[5]

Correspondence to: Thomas J. Meade.

Fax: +1-847-491-3832 tmeade@northwestern.edu.
[‡]These authors contributed equally.

Supporting information for this article is available on the WWW under http://dx.doi.org/10.1002/ejic.201101362.

Supporting Information (see footnote on the first page of this article): ^{1}H NMR, ^{13}C NMR, and mass spectra of synthetic intermediates, HPLC traces of Zn-**1**, Zn-**1**-Eu, and Zn-**1**-Tb, luminescence lifetime measurements of Zn-**1**-Tb, relaxivity plots of Zn-**1**; ^{1}H NMR of Zn titration into **1**-Eu, and T_2 imaging data.

Consequently, these tests cannot differentiate between bacterial infection and sterile inflammation, and are prone to false positive results due to contamination.[6]

As a result, there is a need to develop molecular imaging probes that can specifically identify bacterial infection, monitor therapeutic response, and ultimately guide clinical decisions. Additionally, bacteria-specific contrast agents could aid in the study of infection pathology. Bacteria-targeted imaging probes would allow for in vivo monitoring of both infection progression and antibiotic effectiveness in animal models. This could potentially lead to the development of new antibiotics capable of targeting bacterial strains that have developed resistance to current medications.

To date, several molecular imaging probes have been developed for the specific recognition of bacterial infection. Targeting moieties that have been studied include antibodies,[7] antibiotic drugs,[8] cationic peptides,[9] maltohexose units,[10] and cationic coordination complexes such as Zn^{II} dipicolylamine (Zn-dpa).[11] The interaction between cationic Zn-dpa complexes and bacteria is primarily electrostatic. Zn-dpa groups have a high affinity for the anionic phosphate groups of phospholipids and phosphorylated amphiphiles on the bacterial cell surface.[11e,12] This affinity is affected by the number of Zn-dpa moieties present on the molecule, indicating that cooperative coordination of several targeting groups is involved in binding to the bacterial surface.[11e,12] In contrast to the near-neutral plasma membrane of healthy mammalian cells, which is primarily composed of zwitterionic phospholipids, the phospholipids that compose bacterial membranes are primarily anionic.[13] Thus, Zn-dpa complexes have a high affinity for the negatively-charged bacterial membrane, rendering them selective for bacteria over the neighboring healthy mammalian cells.[11c,11d]

Several optical agents incorporating Zn-dpa groups as bacteria targeting domains have shown promising results both in vitro and in mouse models.[11] However, the inherent limitations of optical imaging, including shallow depth of penetration and surface weighting of images, limit the clinical applicability of such agents.[14] Here we describe the extension of Zn-dpa optical probes for the detection of bacterial infection into the more clinically relevant field of magnetic resonance imaging (MRI). The use of targeted MR contrast agents increases the local concentration of Gd^{III} at the site of interest, enhancing the sensitivity of the probe.[15]

To specifically identify bacterial infection by MRI, two Zn-dpa moieties were conjugated to a Gd^{III} chelate to form the bacteria-targeted MR contrast agent Zn-**1** which has an overall charge of 4+ (see Figures 1 and 2). Previous studies with bacteria-targeted optical agents have indicated that the number of Zn-dpa units affects the labeling efficiency of the compound.[11e] To explore whether this effect is observed for MR agents, two previously published Zn^{II}-binding contrast agents, Zn-**2** and Zn-**3** (Figure 2), were synthesized and examined as control probes.[16] As expected, Zn-**1** was found to bind to *Staphylococcus aureus* (*S. aureus*) to a much greater extent than either Zn-**2** or Zn-**3**. The high affinity of Zn-**1** for bacterial cells permits MR imaging of cells in vitro and suggests the use of Zn-**1** for in vivo detection of bacterial infection.

Results and Discussion

Synthesis of Bacteria-Targeted MRI Contrast Agents

A series of Zn^{II}-binding MR contrast agents composed of a bacteria-targeted Zn^{II}-binding domain conjugated to a Gd^{III} chelate were synthesized (Figure 2). The number and overall charge of the Zn^{II}-binding domains incorporated in the complexes was varied to examine the effect of the derivatives on bacterial cell labeling.

Complexes **2** and **3** were synthesized and characterized as described previously.[16] Both **2** and **3** contain two flexible pendant arms capable of coordinating one Zn^{II} ion. Zn-**3** was used as a control for low-affinity binding to bacteria. The binding domain of **3** is composed of two anionic acetate groups, making the Zn^{II}-bound complex (Zn-**3**) charge neutral. This complex does not possess any electrostatic affinity for the anionic bacterial membrane. In contrast, the binding domain of **2** consists of two neutral picolyl arms, giving the Zn^{II}-bound complex, Zn-**2**, an overall charge of 2+ (Figure 2). The positive charge of the Zn-**2** complex is expected to moderately enhance its affinity for bacteria over Zn-**3**. Previous studies by Smith et al.[11e] have suggested that addition of a second Zn-dpa moiety significantly improves bacteria labeling, leading us to synthesize **1**. This agent contains two dpa groups, each of which is capable of binding one Zn^{II} ion to give the final Zn^{II}-bound complex, Zn-**1**, an overall charge of 4+ (Figure 2).

The synthesis of **1** begins with methylation of the carboxylic acids of 5-hydroxyisophthalic acid to give the diester **4**, in accordance with literature procedures (Scheme 1).[17] The phenol was protected with ethoxymethyl chloride and the esters reduced with lithium aluminum hydride to produce the diol **6**. The alcohol groups were converted to chlorides using trichlorotriazine and DMF to form the dichloride **7**.[18] Displacement of the chlorides with dipicolylamine gave the protected, bis-dpa compound **8**. The phenol was deprotected with trifluoroacetic acid (TFA) in dichloromethane to give **9** in nearly quantitative yield. The bis-dpa phenol **9** was allowed to react with a bromoalkane derivative of tris-*tert*-butyl-protected DO3A to give the final, protected ligand **10**. Deprotection of the *tert*-butyl groups with TFA and subsequent metallation with $Gd(OAc)_3$, yielded the final compound **1**, which was purified by semi-preparative HPLC.

Characterization of Zn-1

Relaxation times (T_1 and T_2) of Zn-**1** suspended in 1.0% (w/v) agarose (all subsequent bacterial samples were suspended in agarose) were measured at 1.41 (37 °C) and 7 T (25 °C) in order to provide data at both clinical and research field strengths. The r_1 increases from 4.7 $mm^{-1}s^{-1}$ to 5.6 $mm^{-1}s^{-1}$ and the r_2 increases from 9.0 $mm^{-1}s^{-1}$ to 21.5 $mm^{-1}s^{-1}$ at 1.41 T and 7 T respectively.

The hydration number, q, of Zn-**1** was determined by comparing the fluorescence lifetimes of the Tb^{III} analogue, Zn-**1**-Tb, in D_2O and H_2O. The fluorescence lifetimes were measured and fit to an exponential curve. The decay times, 1.06 ms in H_2O and 1.89 ms in D_2O, were related to the hydration number using Equation (1), giving a q value of 1.5.[19] The q value is an average measure of how many water molecules are directly bound to the lanthanide at a given time. The non-integer value of 1.5 indicates that that in solution, the complex coordinates either one or two inner sphere water molecules.

$$q = 4.2\left(\frac{1}{\tau_{H_2O}} - \frac{1}{\tau_{D_2O}} - 0.6\right) \quad (1)$$

^1H NMR spectroscopy was used to confirm that **1** binds two Zn^{II} ions per complex. The Eu^{III} analogue of **1** (**1**-Eu) was synthesized and the ^1H NMR chemical shifts of the dpa groups were monitored as Zn^{II} was titrated into solution. The ^1H peaks of the macrocycle and the propylene linker could not be assigned because the peaks are significantly broadened and shifted due to their proximity to the Eu^{III}. However, there is enough separation between the lanthanide and the protons of the Zn^{II}-binding dpa groups to make assignment possible, and a COSY spectrum was acquired to assign the aromatic dpa peaks (Figure 3).

$ZnCl_2$ was added in 0.16 equiv. aliquots until a Zn^{II}:**1**-Eu ratio of 3.82 was obtained. During the titration significant changes in the chemical shift of the dpa protons were observed until a Zn^{II}:**1**-Eu ratio of 2 was reached. The addition of excess Zn^{II} beyond this stoichiometry produced only negligible changes in chemical shift, confirming that **1**-Eu binds two Zn^{II} ions per complex (Figure 4).

In vitro Labeling of Bacteria with MRI Contrast Agents

The relative affinity of Zn-**1**, Zn-**2**, and Zn-**3** for bacteria was determined by quantifying the amount of Gd^{III} bound to bacterial cells after incubation with various concentrations of each contrast agent. The binding affinity was examined for both a Gram-positive strain, *S. aureus*, and a Gram-negative strain, *E. coli* (Figure 5).

Zn-**1** binds readily to *S. aureus* in a dose-dependent manner, with maximum binding occurring at an incubation concentration of 100 μm (Figure 5). However, *S. aureus* incubated with Zn-**2** and Zn-**3** show only minor increases in Gd^{III} content with increasing incubation concentrations, likely due to non-specific binding of the agents to the cell surface. At all incubation concentrations the Gd^{III} content of Zn-**2** and Zn-**3** incubated *S. aureus* is significantly less than cells incubated with Zn-**1**. Specifically, the Gd^{III} content of *S. aureus* incubated with 100 μm Zn-**1** is approximately 16-fold higher than bacteria incubated with 100 μm Zn-**2** and 18-fold higher than bacteria incubated with Zn-**3** (Figure 5).

Interestingly, Zn-**2** does not show an increased affinity for the anionic bacterial membrane despite its positive charge. This suggests that for bacteria-targeted MR contrast agents, the mechanism of interaction between the Zndpa groups and the membrane phospholipids requires the presence of two Zn-dpa moieties, possibly due to a cooperative-binding effect of multiple Zn-dpa moieties on the same molecule coordinating to anionic phosphates on the bacterial surface.[11e,12] We speculate that this cooperative interaction, in addition to the greater charge of the complex, is responsible for the increased affinity of Zn-**1** for *S. aureus*.

In vitro labeling experiments with *E. coli* indicate that Zn-**1** exhibits an affinity for Gram-negative strains; however, the extent of non-specific binding exhibited by Zn-**2** and Zn-**3** is much greater for *E. coli* than *S. aureus*. For lower concentrations of contrast agent (≤ 100 μm), Zn-**1** incubated *E. coli* retains more Gd^{III} than Zn-**2** or Zn-**3** treated cells (Figure 5). Similar to *S. aureus*, the Gd^{III} content of Zn-**1** incubated *E. coli* increases in a concentration-dependent manner and plateaus at 50 μm (contrast agent incubation concentration) whereas the Gd^{III} content of Zn-**2** and Zn-**3** incubated *E. coli* continues to increase even above 50 μm incubation concentrations. This supports the hypothesis that these increases are due to non-specific binding to the surface of *E. coli*.

MR Imaging of Bacterial Cells Labeled with Zn-1, Zn-2, Zn-3

To evaluate the potential of Zn-**1** as a molecular imaging probe, T_1 and T_2 relaxation times of *S. aureus* labeled with Zn-**1**, Zn-**2**, and Zn-**3** were acquired at 1.41 T and 7 T. (T_2 data can be found in the Supporting Information). Bacteria were labeled as described above, using an incubation concentration of 300 μm contrast agent. The samples were washed with LB media and diluted in agarose to create a uniform suspension of bacteria. The T_1-weighted image acquired at 7 T shows significant contrast enhancement in the Zn-**1** labeled sample compared to untreated bacteria; conversely, Zn-**2** and Zn-**3** labeled bacteria show no such contrast enhancement (Figure 6).

At 7 T, the T_1 relaxation time of *S. aureus* cultures labeled with Zn-**1** is approximately 21% lower than the T_1 of untreated cultures. At 1.41 T the reduction in T_1 increases to 44% (Figure 6). Conversely, the T_1 of Zn-**2** and Zn-**3** labeled bacteria is reduced by only 10 and 28% vs. control at 7 T and 1.41 T, respectively (Figure 6).

The pronounced reduction in T_1 relaxation observed at 1.41 T as compared to 7 T may be explained by the field strength dependence of the relationship between rotational correlation time (τ_R) and relaxivity.[20] Binding of MR contrast agents to large macromolecules is known to increase the τ_R, and subsequently the r_1, of contrast agents.[20–21] Zn-**1** is presumed to adhere to the bacterial surface, so it is reasonable to expect both the τ_R and r_1 of the agent to increase upon binding. However, the influence of τ_R on relaxivity is dependent on the field strength; at lower field strengths (i.e. 1.41 T), the effect of τ_R enhancement on relaxivity is more pronounced.[20] Consequently, it is reasonable that bacteria labeled with Zn-**1** exhibit greater decrease in T_1 at lower field strengths.

Equation (1) used to calculate q of Zn-**1**-Tb. τ_{H20} and τ_{D20} are the time constants for the exponential fluorescence decay in H_2O and D_2O, respectively.

Conclusions

We have developed a MR contrast agent (Zn-**1**) that is capable of labeling bacteria cells in vitro. The agent is composed of two cationic, bacteria-targeting Zn^{II}-dpa groups conjugated to a macrocyclic Gd^{III} complex. NMR studies confirm that each dpa group on the complex binds one Zn^{II} ion, giving the final Zn-**1** complex an overall charge of 4+.

Zn-**1** shows a dose-dependent affinity for *S. aureus* nearly 20 times higher than the charge neutral control compound Zn-**3**. The low labeling efficiency of Zn-**2**, a contrast agent containing only one Zn-dpa group, indicates that the interaction between the Zn-dpa groups of Zn-**1** and the anionic phosphate groups of the bacterial membrane require the presence of two Zn-dpa groups for effective binding. The reduction in the T_1 relaxation time of bacteria labeled with Zn-**1** corresponds to a significant contrast enhancement at 7 T, though as expected is more pronounced at lower field strengths, verifying the potential of Zn-**1** as an in vivo MR probe for detection of bacterial infection.

Experimental Section

Bacterial Culture

Staphylococcus aureus (29213) and *Escherichia coli* K-12 (29425) were obtained from ATCC (Rockville, MD). Bacteria were grown from glycerol stocks, cultured in Luria–Bertani (LB) growth media with agitation overnight at 37 °C. All experiments were performed after the bacteria had reached stationary phase to ensure that bacterial growth did not affect labeling efficiency. The optical density at 600 nm (OD_{600}) was measured before and after labeling to confirm that the number of bacteria did not change significantly during the course of the experiment.

Synthesis of Zn-1

Chloromethyl ethyl ether and 2,2'-dipicolylamine were obtained from TCI America. All other chemicals were obtained from Sigma Aldrich and used without further purification. EMD 60F 254 silica gel plates were used for thin layer chromatography and visualized using UV light, iodoplatinate stain, or cerium ammonium molybdate (CAM) stain. Column chromatography was performed using standard grade 60 Å 230–400 mesh silica gel (Sorbent Technologies). Unless otherwise noted, ^1H and ^{13}C NMR were obtained on a Bruker Avance III 500 MHz NMR Spectrometer. A Varian 1200 L single-quadrupole mass

spectrometer was used to acquire electrospray ionization mass spectra (ESI-MS). Semi-preparative HPLC was performed on a Waters 19 × 250 mm Atlantis C18 Column. Analytical HPLC-MS was performed using a Waters 4.6 × 250 mm 5 μm Atlantis C18 column using the Varian Prostar 500 system equipped with a Varian 380 LC ELSD system, a Varian 363 fluorescence detector, and a Varian 335 UV/Vis detector. ^{1}H NMR of **1**-Eu as a function of Zn^{II} concentration was performed on a Bruker Avance III 600 MHz spectrometer at 60 °C in d_6-DMSO.

Dimethyl 5-hydroxyisophthalate **(4)** was synthesized according to literature procedure.[17]

Dimethyl 5-(Ethoxymethoxy)isophthalate (5)

To a solution of **4** (4.42 g, 21 mmol) in acetone (50 mL) was added K_2CO_3 (11.5 g, 84 mmol). The reaction was cooled to 0 °C, and chloromethylethyl ether (2.74 g, 29 mmol) was added. After 12 h, TLC (30% ethyl acetate/hexanes) confirmed completion of the reaction. The reaction mixture was filtered and the solvent evaporated. The residue was purified on a silica gel column, eluting with 15% ethyl acetate/hexanes, to give 4.72 g of product as a white solid (84% yield). ^{1}H NMR (500 MHz, $CDCl_3$): δ = 8.29 (t, J = 1.5 Hz, 1 H, H_{aryl}), 7.84 (d, J = 1.5 Hz, 2 H, H_{aryl}), 5.27 (s, 2 H, O-CH_2-O), 3.91 (s, 6 H, O-CH_3), 3.71 (q, J = 7.0 Hz, 2 H, CH_2CH$_3$), 1.19 (t, J = 7.1 Hz, 3 H, CH$_2$CH_3) ppm. ^{13}C NMR (126 MHz, $CDCl_3$): δ = 166.08 (COOMe), 157.38 (C_{ar}-OCH$_2$), 131.83 (C_{ar}-COOMe), 124.00 (C_{ar}), 121.55 (C_{ar}), 93.14 (O-CH$_2$-O), 64.68 (CH$_2$-CH$_3$), 52.48 (COO-CH$_3$), 15.12 (CH$_3$) ppm.

[5-(Ethoxymethoxy)-1,3-phenylene]dimethanol (6)

Lithium aluminum hydride (1.22 g, 32.8 mmol) was suspended in THF (50 mL), and the mixture cooled to 0 °C. A solution of **5** (4 g, 14.9 mmol) in THF (40 mL) was added dropwise to the LAH suspension. After 2 h, completion of the reaction was confirmed by TLC (5% MeOH/DCM). The reaction was quenched with 15 mL of water. The reaction mixture was filtered and the solvent evaporated. The residue was brought up in ethyl acetate and washed with water and brine. The organic layer was dried with Na_2SO_4, filtered, and the solvent evaporated to give 2.63 g of product as a white, oily solid (83% yield). ^{1}H NMR (500 MHz, $CDCl_3$): δ = 6.99 (s, 1 H, H_{ar}), 6.94 (d, J = 1.4 Hz, 2 H, H_{ar}), 5.22 (s, 2 H, O-CH_2-O), 4.64 (d, J = 3.7 Hz, 4 H, CH_2-OH), 3.72 (q, J = 7.0 Hz, 2 H, CH_2CH$_3$), 2.15 (s, 2 H, OH), 1.22 (t, J = 7.1 Hz, 3 H, CH CH_3) ppm. ^{13}C NMR (126 MHz, $CDCl_3$): δ = 157.85 (C_{ar}-OCH$_2$), 142.97 (C_{ar}-CH$_2$OH), 118.73 (C_{ar}), 113.92 (C_{ar}), 93.15 (O-CH$_2$-O), 65.15 (CH$_2$-OH), 64.51 (CH$_2$CH$_3$), 15.23 (CH$_2$-CH$_3$) ppm.

1,3-Bis(chloromethyl)-5-(ethoxymethoxy)benzene (7)

Trichlorotriazine (4.35 g, 23.58 mmol) was dissolved in DMF (10 mL) at room temperature and allowed to stir for one hour until the formation of a yellow precipitate was observed. A solution of **6** (2 g, 9.43 mmol) in DCM (30 mL) was added and the reaction allowed to stir overnight at room temperature. After confirming completion of the reaction by TLC (15% ethyl acetate/hexanes), the reaction mixture was transferred to a separatory funnel and washed successively with water, a saturated solution of Na_2CO_3, and brine. The organics were dried with Na_2SO_4, filtered and the solvent evaporated. The residue was adsorbed to silica and purified on a silica gel column, eluting with 5% ethyl acetate/hexanes to give 1.29 g of product as a clear oil (55% yield). ^{1}H NMR (500 MHz, $CDCl_3$): δ = 7.06 (d, J = 1.5 Hz, 1 H, H_{ar}), 7.03 (d, J = 1.6 Hz, 2 H, H_{ar}), 5.24 (s, 2 H, O-CH_2-O), 4.54 (s, 4 H, CH_2-Cl), 3.73 (q, J = 7.1 Hz, 2 H, CH_2-CH$_3$), 1.23 (t, J = 7.1 Hz, 3 H, CH$_2$-CH_3) ppm. ^{13}C NMR (126 MHz, $CDCl_3$): δ = 157.85 (C_{ar}-OCH$_2$), 139.38 (C_{ar}-CH$_2$Cl), 121.96 (C_{ar}), 116.37 (C_{ar}), 93.15 (O-CH_2-O), 64.46 (CH$_2$CH$_3$), 45.76 (CH$_2$Cl), 15.13 (CH$_2$$CH_3$) ppm.

[5-(Ethoxymethoxy)benzene-1,3-diyl]bis[*N*,*N*-bis(pyridin-2-ylmethyl)methanamine] (8)

DIEA (1.74 g, 13.5 mmol) and 2,2'-dipicolylamine were stirred in DCM (10 mL) for 10 min. A solution of **7** in DCM (10 mL) was added and the reaction allowed to stir at room temperature. After 4 d, completion of the reaction was confirmed by MS. The solvent was evaporated and the residue purified on a silica column eluting with 4 % methanol/chloroform to give 3.5 g of product as a yellow oil (99% yield). ^{1}H NMR (500 MHz, $CDCl_3$): δ = 8.48 (dd, J = 3.8, 2.3 Hz, 4 H, *o*-H_{py}), 7.66–7.54 (m, 8 H, H_{py}), 7.11 [td, J = 5.1, 3.3 Hz, 5 H, H_{py} (4 H), H_{ar} (1 H)], 7.02 (d, J = 1.4 Hz, 2 H, H_{ar}), 5.20 (s, 2 H, O-CH_2-O), 3.78 (s, 8 H, N-CH_2-C_{py}), 3.71 (q, J = 7.1 Hz, 2 H, CH_2-CH_3), 3.63 (s, 4 H, C_{ar}-CH_2-N), 1.19 (t, J = 7.1 Hz, 3 H, CH_2CH_3) ppm. ^{13}C NMR (126 MHz, $CDCl_3$): δ = 159.88 (CH_2-*o*-C_{py}-N_{py}), 157.74 (C_{ar}-OCH_2), 149.02 (*o*-C_{py}-N_{py}), 140.85 (C_{ar}-CH_2N), 136.53 (*c*-C_{py}), 122.78 (*m*-C_{py}), 122.44 (C_{ar}), 122.04 (*m*-C_{py}), 115.12 (C_{ar}), 93.32 (O-CH$_2$-O), 64.27 (CH$_2$CH$_3$), 60.16 (N-CH$_2$-C_{py}), 58.57 (C_{ar}-CH$_2$-N), 15.26 (CH_2CH$_3$) ppm. MS (ESI-positive): m/z = 575.3 [M^+], 597.3 [M + Na^+].

3,5-Bis{[bis(pyridin-2-ylmethyl)amino]methyl}phenol (9)

A solution of **8** (2.21 g, 3.84 mmol) in DCM was heated to 40 °C. Trifluoroacetic acid (2.38 mL, 23 mmol) was added and the reaction allowed to stir for 12 h (monitored by TLC: 10% methanol/DCM). The protonated product was extracted from DCM with water. The aqueous layer was neutralized and the product extracted into DCM. The organic layers were combined, dried with Na_2SO_4, filtered and the solvent evaporated to give 1.73 g of product as a yellow oil. ^{1}H NMR (500 MHz, $CDCl_3$): δ = 8.52–8.40 (m, 4 H, *o*-H_{py}), 7.65–7.54 (m, 8 H, H_{py}), 7.12 (td, J = 5.7, 2.4 Hz, 4 H, H_{py}), 7.02 (s, 1 H, H_{ar}), 6.79 (d, J = 1.2 Hz, 2 H, H_{ar}), 3.77 (s, 8 H, CH_2-C_{py}), 3.56 (s, 4 H, C_{ar}-CH_2-N), 2.60–2.20 (m, 1 H, OH) ppm. ^{13}C NMR (126 MHz, $CDCl_3$): δ = 159.88 (CH_2-C_{py}-N_{py}), 157.57 (C_{ar}-OH), 148.80 (*o*-C_{py}), 140.74 (C_{ar}-CH_2N), 136.86 (*p*-C_{py}), 123.03 (*m*-C_{py}), 122.24 (*m*-C_{py}), 120.07 (C_{ar}), 114.86 (C_{ar}), 60.05 (N-CH$_2$-C_{py}), 58.77 (C_{ar}-CH$_2$-N) ppm. MS (ESI-positive): m/z = 517.2 [M^+], 539.2 [M + Na^+].

Tri-*tert*-butyl 10-[3-(3,5-Bis{[bis(pyridin-2-ylmethyl)amino]methyl}-phenoxy)propyl]-1,4,7,10-tetraazacyclododecane-1,4,7-tricarboxylate (10)

Tri-*tert*-butyl 10-(3-bromopropyl)-1,4,7,10-tetraazacyclododecane-1,4,7-tricarboxylate (tris-*tert*-butyl-DO3A) was synthesized by reacting tris-*tert*-butyl-DO3A with a large excess of 1,3-dibromopropane. K_2CO_3 (1.85 g, 13.48 mmol) and dibromopro-pane (3.4 mL, 30.36 mmol) were dissolved in acetonitrile (400 mL) and cooled to 0 °C. Tris-*tert*-butyl-DO3A (2 g, 3.36 mmol), synthesized according to literature procedure, was dissolved in acetonitrile (50 mL) and added to the above solution via dropping funnel. Reaction progress was monitored by MS. After three days the reaction was filtered, the solvent evaporated, and the crude product run on a silica gel column, eluting with 2–4% methanol in DCM. The bromopropyl-DO3A was added to a solution of K_2CO_3 (1.25 g, 9.05 mmol) and **9** (937 mg, 1.81 mmol) in acetonitrile (60 mL). The reaction was heated to 70 °C and allowed to reflux under nitrogen for 48 h. The reaction mixture was filtered and the solvent evaporated. The crude product was purified on a silica gel column, eluting with 7–10% methanol in chloroform to give 460 mg of yellow oil (25% yield). ^{1}H NMR (500 MHz, $CDCl_3$): δ = 8.51 (dt, J = 4.9, 1.4 Hz, 4 H, *o*-H_{py}), 7.75–7.52 (m, 8 H, H_{py}), 7.15 [ddd, J = 6.9, 4.8, 1.5 Hz, 5 H, 4 H_{py} (4 H), H_{ar} (1 H)], 6.75 (d, J = 1.5 Hz, 2 H, H_{ar}), 3.92 (s, 2 H, CH_2-CH_2-OH), 3.79 (s, 8 H, N-CH_2-C_{py}), 3.64 (s, 4 H, C_{ar}-CH_2-N), 3.41–1.80 [m, 26 H, N-CH_2-CH_2-N (16 H), N-CH_2-COOH (6 H), N-CH_2-CH_2-CH_2 (4 H)], 1.44 (d, J = 9.8 Hz, 27 H) ppm. ^{13}C NMR (126 MHz, $CDCl_3$): δ = 172.68 (*C*OO-*t*Bu), 171.77 (*C*OO-*t*Bu), 158.68 (CH_2-C_{py}-N_{py}), 157.96 (C_{ar}-OCH_2), 148.01 (*o*-C_{py}), 139.57 (C_{ar}-CH_2-N), 135.56 (*p*-C_{py}), 121.76 (*m*-C_{py}), 121.10 (*m*-C_{py}), 120.50 (C_{ar}), 112.46 (C_{ar}), 81.76 (O-*C*-CH_3), 81.45 (O-*C*-CH_3), 80.91 (O-

C-CH_3), 65.29 (O-*C*H_2-CH_2), 59.03 (N-*C*H_2-C_{py}), 57.65 (C_{ar}-*C*H_2-N), 55.64 (N-*C*H_2-*C*H_2-N), 54.86 (N-*C*H_2-*C*H_2-N), 49.48 (N-*C*H_2-COOH), 27.17 (C-*C*H_3), 27.03 (C-*C*H_3), 26.87 (C-*C*H_3), 25.18 (CH_2-*C*H_2-CH_2) ppm. MS (ESI-positive): *m/z* = 1071 [M^+], 1093 [M + Na^+], 547.6 [(M^+ + Na^+)/2], 558.3 [(M + 2Na^+)/2], 573.4 [(M + Na^+ + K^+)/2], 595.3 [(M + 3K^+)/2].

Bis-dpa-Gd (1)

The protected ligand **10** (338 mg, 0.315 mmol) was dissolved in a mixture of 95:2.5:2.5 TFA/triisopropylsilane/water and allowed to stir for four hours. The acid was evaporated under nitrogen. Removal of the *tert*-butyl protecting groups was confirmed by ESI-MS. The residue was brought up in water (5 mL) and the pH adjusted to 6.5 with NaOH (1 m). $Gd(OAc)_3$ 6 H_2O (148 mg, 0.47 mmol) was added, and the solution allowed to stir at 50 °C for 4 d, adjusting the pH back to 6.5 with NaOH (1 m) as needed. The product was purified with reverse phase semi-preparative HPLC using a C18 column and eluting with a gradient of 0– 100% acetonitrile in water over 35 min, t_r = 23 min. The purity and identity of the product was confirmed using analytical HPLC-MS on a C18 column, eluting with a gradient of 20–100% acetonitrile in water over 35 min, t_r = 19.5 min. The solvent was evaporated from pure fractions, and the residue brought up in DMSO and freeze dried. MS (ESI-positive) *m/z* = 1058.3 [M^+], 530.6 [M^{2+}/2].

Bis-dpa-Eu (1-Eu)

The same procedure was followed as for **1**, using $EuCl_3$·6H_2O for metallation. Retention times were the same as for **1**. MS (ESI-positive): *m/z* = 1053.2 [M^+] 527.2 [M^{2+}/2].

Bis-dpa-Tb (1-Tb)

The same procedure was followed as for **1**, using $Tb(OAc)_3$·6H_2O for metallation. Retention times were the same as for **1**. MS (ESI-positive): *m/z* = 1059.2 [M^+] 530.2 [M^{2+}/2].

Luminesence Lifetime Measurements

The luminescence lifetime of a 200 mm solution of Zn-**1**-Tb was measured H_2O and D_2O on a Hitachi (San Francisco, CA) F4500 fluorimeter, using a λ_x = 254 nm and λ_{em} = 544 nm. Twenty-five scans were acquired, averaged and fit to a monoexponential decay function.

Quantification of Bacterial Cell Labeling by Inductively Coupled Plasma Mass Spectrometry (ICP-MS)

Stock solutions (1 mm) of **1**, **2**, and **3** were prepared by dissolving each contrast agent in a solution of 2% DMSO in LB media. One molar equivalent of $ZnCl_2$ was added to **2** and **3**, while two molar equivalents of $ZnCl_2$ were added to **1**. The solutions were incubated at room temperature for 20 min (to form the Zn^{II}-bound complexes), and were placed in a sonicating water bath (Branson 5510; Branson Ultrasonics, Danbury, CT) for an additional 10 min to ensure that all material was dissolved. The stock solutions were diluted to the desired concentrations with LB media.

S. aureus or *E. coli* cells were grown from a glycerol stock in LB media overnight. One mL aliquots of bacteria were taken and centrifuged at 6000 *g* for 3 min. The bacterial cell pellets were re-suspended in various concentrations of Zn-**1**, Zn-**2** or Zn-**3** and allowed to incubate at room temperature for 1 h while rotating. Bacteria were then centrifuged at 6000 *g* for 3 min, the supernatant was decanted, and the bacterial cell pellets were re-suspended in 1 mL LB media. This was repeated two more times for a total of three washes to remove any unbound contrast agent and decrease non-specific binding.

After washing, quantification of gadolinium was accomplished using inductively coupled plasma mass spectrometry (ICP-MS) of acid-digested samples. Specifically, bacterial cell pellets were digested in 100 μL of concentrated nitric acid (> 69%, Sigma, St. Louis, MO, USA) and placed at 70 °C for at least 12 h to allow for complete sample digestion. Ultra pure H_2O (18.2 MΩ·cm) and multi-element internal standard containing Bi, Ho, In, Li(6), Sc, Tb, and Y (CLISS-1, Spex Certiprep, Metuchen, NJ, USA) were then added to produce a final solution of 3.0% nitric acid (v/v) and 5.0 ng/mL internal standard up to a total sample volume of 10 mL. Samples were then syringe filtered using 0.2 μm polyamide filters (Macherey–Nagel, Germany) into new 15 mL conical tubes. Individual Gd elemental standards were prepared at 1.00, 5.00, 10.0, 25.0, 50.0, 100, and 250 ng/mL concentrations with 3.0% nitric acid (v/v) and 5.0 ng/mL internal standards up to a total sample volume of 25 mL (using volumetric flasks).

ICP-MS was performed on a computer-controlled (Plasmalab software) Thermo X series II ICP-MS (Thermo Fisher Scientific, Waltham, MA, USA) equipped with a CETAC 260 autosampler (Omaha, NE, USA). Each sample was acquired using 1 survey run (10 sweeps) and 3 main (peak jumping) runs (100 sweeps). The isotopes selected for analysis were ^{157,158}Gd, and ^{115}In and ^{165}Ho (chosen as internal standards for data interpolation and machine stability).

Relaxation Time Measurements at 1.41 T

T_1 and T_2 relaxation times were measured on a Bruker mq60 NMR analyzer equipped with Minispec v. 2.51 Rev.00/NT software (Billerica, MA, USA) operating at 1.41 T (60 MHz) and 37 °C. T_1 relaxation times were measured using an inversion recovery pulse sequence (t1_ir_mb) with the following parameters: four scans per point, 10 data points for fitting, mono-exponential curve fitting, phase cycling, 10 ms first pulse separation, and a recycle delay and final pulse separation ≥ 5 T_1. T_2 relaxation times were measured using a Carr–Purcell–Meiboom–Gill (CPMG) pulse sequence (t2_cp_mb) with the following parameters: four scans per point, mono-exponential curve fitting, phase cycling, 10 ms first pulse separation, 15 second recycle delay, 1 ms 90°–180° pulse separation (tau), while altering the number of data points to ensure accurate mono-exponential curve fitting (500–10000 data points for fitting). Relaxivities were determined by taking the slope of a plot of $1/T_1(s^{-1})$ or $1/T_2(s^{-1})$ vs. gadolinium concentration (mM) of each compound in either LB broth or in 1% (w/v) agarose.

MR Imaging and Relaxation Time Measurements at 7.05 T

All MR imaging was performed on an 89 mm bore size PharmaScan 7.05 T MR imaging spectrometer fitted with shielded gradient coils (Bruker BioSpin, Billerica, MA, USA) using a RF RES 300 1H 089/023 quadrature transmit/receive mouse brain volume coil (Bruker BioSpin, Billerica, MA, USA). All MR images were acquired using Paravision 5.0.1 software (Bruker BioSpin, Billerica, MA, USA).

S. aureus cultures were labeled with 300 μM Zn-**1**, Zn-**2**, and Zn-**3** and then washed three times the LB broth as described previously. After the final wash samples were centrifuged at 6000 *g* for 3 min to pellet the bacteria, which were then suspended in 1.0 % (w/v) low melting point agarose (Sigma, St. Louis, MO) in 7.5 mm outer diameter NMR tubes and incubated on ice to allow for gelation of the agarose. Samples were then positioned in a 23 mm mouse brain volume transmit/receive coil prior to imaging.

T_1-weighted images were acquired using a rapid-acquisition rapid-echo variable-repetition time (RAREVTR) pulse sequence using the following parameters: RARE factor: 1, echo time (TE): 11 ms, averages: 3, matrix size (MTX): 128 × 128, field of view (FOV): 25 × 25

mm^2, 6 slices, slice thickness: 1.5 mm, interslice distance: 2.0 mm, repetition times, TR = 15000, 10000, 8000, 6000, 3000, 1500, 1000, 750, 500, 300, 200, and 150 ms, and a total scan time of ca. 3 h 45 min. T_1 values of selected regions of interest (ROIs) of 5 out of 6 slices were calculated using the T_1 saturation recovery mono-exponential curve fitting formula provided by the image sequence analysis (ISA) tool in Paravision 5.0.1 software (Bruker BioSpin, Billerica, MA, USA).

Color T_1 maps were generated using using Jim v. 6.0 software (Xinapse Systems Ltd., Aldwincle, UK). Briefly, the desired ROIs were masked using the contour ROI function T_1 maps were then generated using the saturation-recovery T_1 fit function in the image-least-squares fitter entering TRs in the single input image configuration. Color maps were generated using an inverted rainbow color lookup table setting the maximum T_1 to 3000 ms. Images were processed using the image resampler by resizing pixels to smooth the image by converting a 128 × 128 MTX to 384 × 384 MTX (changing the number of columns and rows under pixel resizing specifications).

T_2-weighted images were acquired using a multi-slice multi-echo (MSME) pulse sequence with variable echo times using the following parameters: TR = 6000 ms, averages: 3, MTX = 128 × 128, FOV = 25 × 25 mm^2, 6 slices, slice thickness: 1.5 mm, interslice distance: 2.0 mm, TE = 11, 22, 33, 44, 55, ... 352 ms, and a total scan time of ca. 29 min. T_2 values of selected regions of interest (ROIs) of 5 out of 6 slices were calculated using a T_2 mono-exponential decay curve fitting formula provided by the image sequence analysis (ISA) tool in Paravision 5.0.1 software (Bruker BioSpin, Billerica, MA, USA).

Color T_2 maps were generated using using Jim v. 6.0 software (Xinapse Systems Ltd., Aldwincle, UK). Briefly, the desired ROIs were masked using the contour ROI function T_2 maps were then generated using the single-exponential T_2 decay fit function in the image-least-squares fitter entering TEs in the single input image configuration. Color maps were generated using an inverted rainbow color lookup Table setting the maximum T_2 to 200 ms and the minimum T_2 to 75 ms. Images were processed using the image resampler by resizing pixels to smooth the image by converting a 128 × 128 MTX to 384 × 384 MTX (changing the number of columns and rows under pixel resizing specifications).

Supplementary Material

Refer to Web version on PubMed Central for supplementary material.

Acknowledgments

The authors gratefully acknowledge Daniel Mastarone for assistance with NMR experiments. This work was generously supported by the National Institutes of Health (NIH) (grant nuber R01EB005866). Imaging work was performed at the Northwestern University Center for Advanced Molecular Imaging generously supported by the National Cancer Institute Cancer Center Support Grant (NCI CCSG P30 CA060553 awarded to the Robert H. Lurie Comprehensive Cancer Center). MRI was performed on the 7 T Bruker Pharmascan system purchased with the support of the National Center for Research Resources (NCRR) (grant number 1S10RR025624-01). NMR studies were completed at the Northwestern University Integrated Molecular Structure Education and Research Center. A description of the facility and full funding dis closure can be found at http://pyrite.chem.northwestern.edu/analyticalserviceslab/asl.htm. Metal analysis was performed at the Northwestern University Quantitative Bioelemental Imaging Center generously supported by the NASA Ames Research Center (grant number NNA04CC36G). L. M. M. acknowledges support from the National Science Foundation Graduate Research Fellowship. A. S. H. acknowledges support from the Natural Sciences and Engineering Research Council of Canada for a post-graduate fellowship.

References

1. Singh A, Goering RV, Simjee S, Foley SL, Zervos MJ. Clin. Microbiol. Rev. 2006; 19:512–530. [PubMed: 16847083]
2. a Caly WR, Strauss E. J. Hepatol. 1993; 18:353–358. [PubMed: 8228129] b Kollef MH, Sherman G, Ward S, Fraser VJ. Chest. 1999; 115:462–474. [PubMed: 10027448] c Rayes N, Seehofer D, Theruvath T, Schiller Reinhold A, Langrehr Jan M, Jonas S, Bengmark S, Neuhaus P. Am. J. Transplant. 2005; 5:125–130. [PubMed: 15636620]
3. a Aydinuraz K, Ağalar C, Ağalar F, Çeken S, Duruyürek N, Vural T. J. Surg. Res. 2009; 157:e79–e86. [PubMed: 19592038] b Ben, H. Chew; Lange, D. Nat. Rev. Urol. 2009; 6:440–448. [PubMed: 19597512]
4. Hirsch Elizabeth B, Tam Vincent H. Expert Rev. Pharmacoecon Outcomes Res. 2010; 10:441–451. [PubMed: 20715920]
5. Pourakbari B, Mamishi S, Zafari J, Khairkhah H, Ashtiani MH, Abedini M, Afsharpaiman S, Rad SS. Braz. J. Infect. Dis. 2010; 14:252–255. [PubMed: 20835508]
6. Pien BC, Sundaram P, Raoof N, Costa SF, Mirrett S, Woods CW, Reller LB, Weinstein MP. Am. J. Med. 2010; 123:819–828. [PubMed: 20800151]
7. Wang L, Zhao W, O'Donoghue Meghan B, Tan W. Bioconjugate Chem. 2007; 18:297–301.
8. Zhang S, Zhang W, Wang Y, Jin Z, Wang X, Zhang J, Zhang Y. Bioconjugate Chem. 2011; 22:369–375.
9. Brouwer CPJM, Sarda-Mantel L, Meulemans A, Le Guludec D, Welling MM. Mini-Rev. Med. Chem. 2008; 8:1039–1052. [PubMed: 18782056]
10. Ning X-H, Lee S-J, Wang Z-R, Kim D-I, Stubblefield B, Gilbert E, Murthy N. Nat. Mater. 2011; 10:602–607. [PubMed: 21765397]
11. a Leevy WM, Gammon ST, Johnson JR, Lampkins AJ, Jiang H, Marquez M, Piwnica-Worms D, Suckow MA, Smith BD. Bioconjugate Chem. 2008; 19:686–692.b DiVittorio KM, Leevy WM, O'Neil EJ, Johnson JR, Vakulenko S, Morris JD, Rosek KD, Serazin N, Hilkert S, Hurley S, Marquez M, Smith BD. ChemBioChem. 2008; 9:286–293. [PubMed: 18076009] c Leevy WM, Johnson JR, Lakshmi C, Morris J, Marquez M, Smith BD. Chem. Commun. 2006:1595–1597.d Leevy WM, Gammon ST, Jiang H, Johnson JR, Maxwell DJ, Jackson EN, Marquez M, Piwnica-Worms D, Smith BD. J. Am. Chem. Soc. 2006; 128:16476–16477. [PubMed: 17177377] e Lakshmi C, Hanshaw RG, Smith BD. Tetrahedron. 2004; 60:11307–11315.
12. Surman AJ, Bonnet CS, Lowe MP, Kenny GD, Bell JD, Toth E, Vilar R. Chem. Eur. J. 2011; 17:223–230. S223/221–S223/216. [PubMed: 21207619]
13. Koga Y. J. Mol. Evol. 2011; 72:274–282. [PubMed: 21259003]
14. Jaffer FA, Weissleder R. JAMA J. Am. Med. Assoc. 2005; 293:855–862.
15. a Sukerkar PA, MacRenaris KW, Meade TJ, Burdette JE. Mol. Pharm. 2011; 8:1390–1400. [PubMed: 21736390] b Sukerkar PA, MacRenaris KW, Townsend TR, Ahmed RA, Burdette JE, Meade TJ. Bioconjugate Chem. 2011; 22:2304–2316.
16. a Major JL, Boiteau RM, Meade TJ. Inorg. Chem. 2008; 47:10788–10795. [PubMed: 18928280] b Major JL, Parigi G, Luchinat C, Meade TJ. Proc. Natl. Acad. Sci. USA. 2007; 104:13881–13886. [PubMed: 17724345]
17. Ashton PR, Anderson DW, Brown CL, Shipway AN, Stoddart JF, Tolley MS. Chem. Eur. J. 1998; 4:781–795.
18. De Luca L, Giacomelli G, Porcheddu A. Org. Lett. 2002; 4:553–555. [PubMed: 11843589]
19. Quici S, Cavazzini M, Marzanni G, Accorsi G, Armaroli N, Ventura B, Barigelletti F. Inorg. Chem. 2005; 44:529–537. [PubMed: 15679381]
20. a Strauch RC, Mastarone DJ, Sukerkar PA, Song Y, Ipsaro JJ, Meade TJ. J. Am. Chem. Soc. 2011; 133:16346–16349. [PubMed: 21942425] b Hermann P, Kotek J, Kubicek V, Lukes I. Dalton Trans. 2008:3027–3047. [PubMed: 18521444]
21. a Manus LM, Mastarone DJ, Waters EA, Zhang X-Q, Schultz-Sikma EA, MacRenaris KW, Ho D, Meade TJ. Nano Lett. 2010; 10:484–489. [PubMed: 20038088] b Song Y, Xu X, MacRenaris KW, Zhang X-Q, Mirkin CA, Meade TJ. Angew. Chem. 2009; 121:9307.Angew. Chem. Int. Ed. 2009; 48:9143–9147. S9143/9141–S9143/9124.c Song Y, Kohlmeir EK, Meade TJ. J. Am. Chem. Soc.

2008; 130:6662–6663. [PubMed: 18452288] d Cilliers R, Song Y, Kohlmeir EK, Larson AC, Omary RA, Meade TJ. Magn. Reson. Med. 2008; 59:898–902. [PubMed: 18383280]

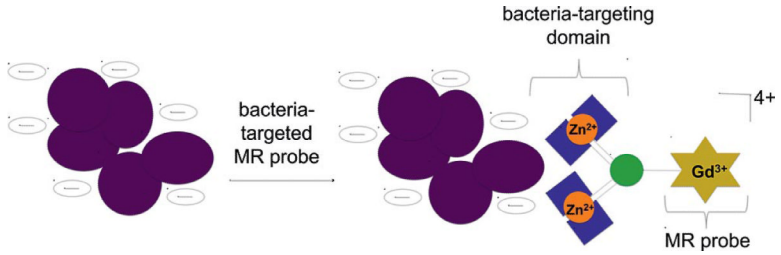

Figure 1.

Two bacteria-targeted Zn-dpa domains were conjugated to a macrocyclic Gd^{III} chelate to develop a bacteria-targeted MR probe. The probe's affinity for bacteria is due to the electrostatic attraction between the anionic bacteria membrane and the positive charge of the Zn-dpa moieties.

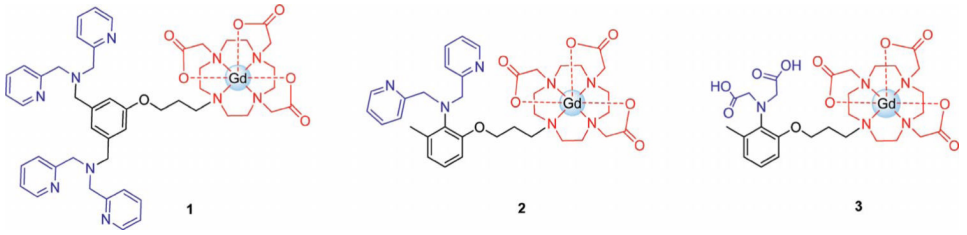

Figure 2.

Structures of complexes used for bacteria labeling studies. The Zn^{II}-binding domains of the complexes are shown in blue, the Gd^{III} chelate is shown in red. After the addition of Zn^{II}, Zn-**1** and Zn-**2** have charges of 4+ and 2+, respectively, while Zn-**3** is charge neutral.[16] The positive charge of Zn-**1** and Zn-**2** is expected to enhance the complex's affinity for anionic bacterial cell membranes. Zn-**3** was used as a control for low-affinity binding.

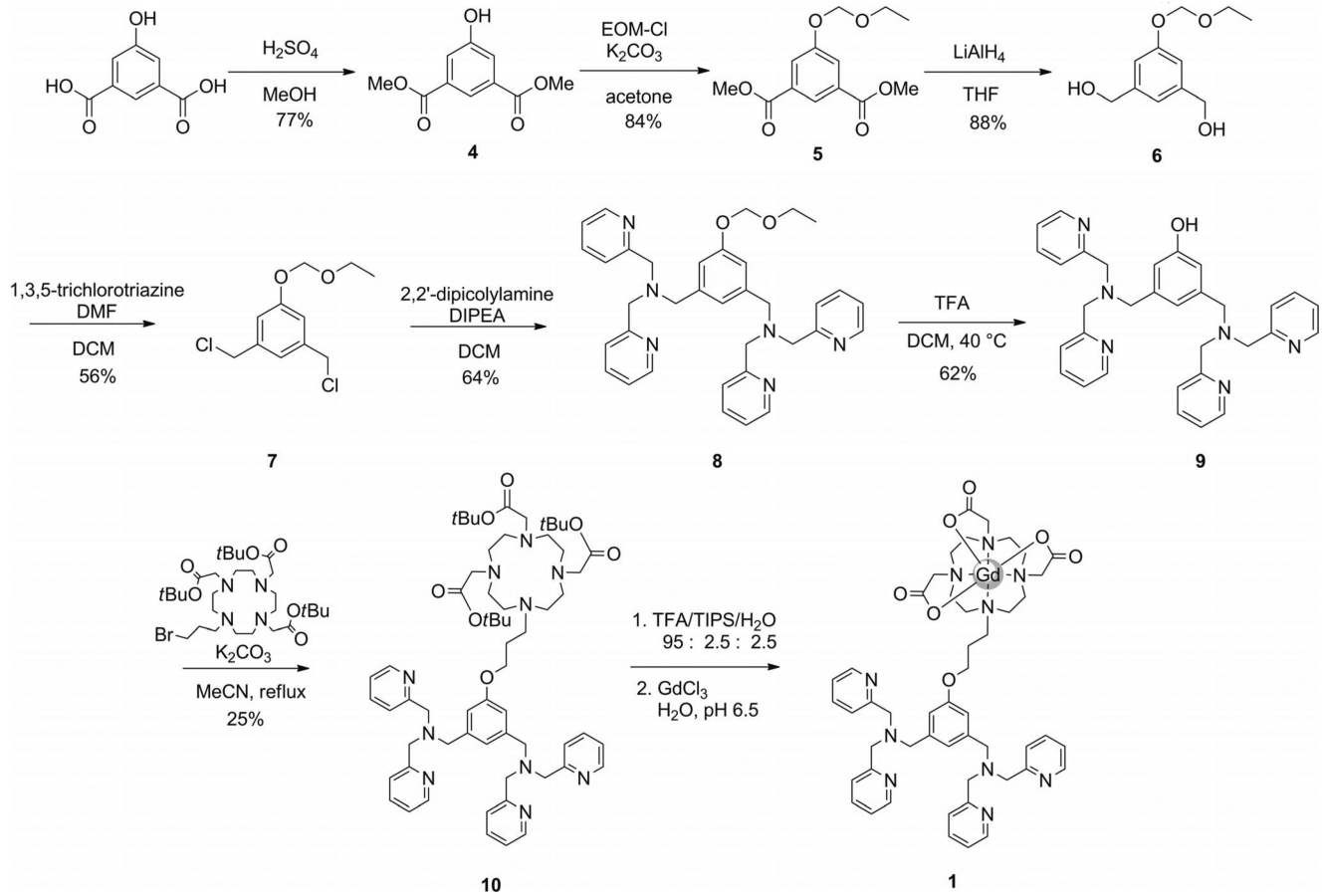

Scheme 1.

Synthesis of the bacteria-targeted MR contrast agent **1** that contains two dipicolyl moieties, each of which is capable of binding one Zn^{II} ion to give the final Zn^{II}-bound complex an overall charge of 4+. The europium and terbium analogues were synthesized in a similar manner, using $EuCl_3$ and $Tb(OAc)_3$ in place of $Gd(OAc)_3$.

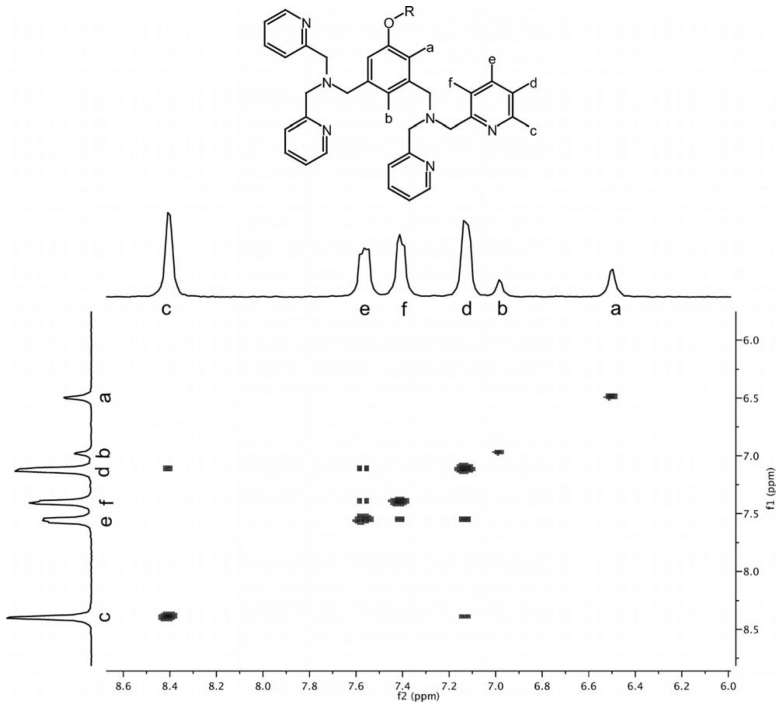

Figure 3.

Aromatic region of **1**-Eu COSY spectrum (60 °C, DMSO) used to assign peaks of the Zn^{II} binding domains of **1**. The addition of Zn^{II} produces significant changes in the chemical shift of the protons on the Zn^{II} binding domain until a Zn^{II}:**1**-Eu ratio of 2 is reached.

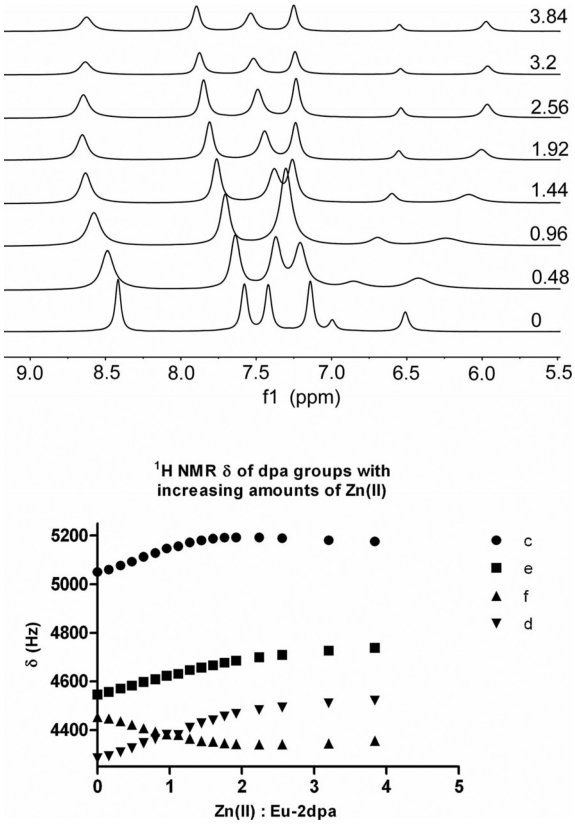

Figure 4.

Top: aromatic region of ^{1}H NMR spectrum of Eu-**1** with increasing amounts of Zn^{II}. Bottom: Chemical shift of peaks c, e, f, and d (see Figure 3) as a function of Zn^{II}/Eu-**1** ratio. It is clear that the peaks of the Zn^{II} binding domain shift only until a Zn^{II}/Eu-**1** ratio of 2 is obtained, confirming that each Eu-**1** binds two Zn^{II} ions.

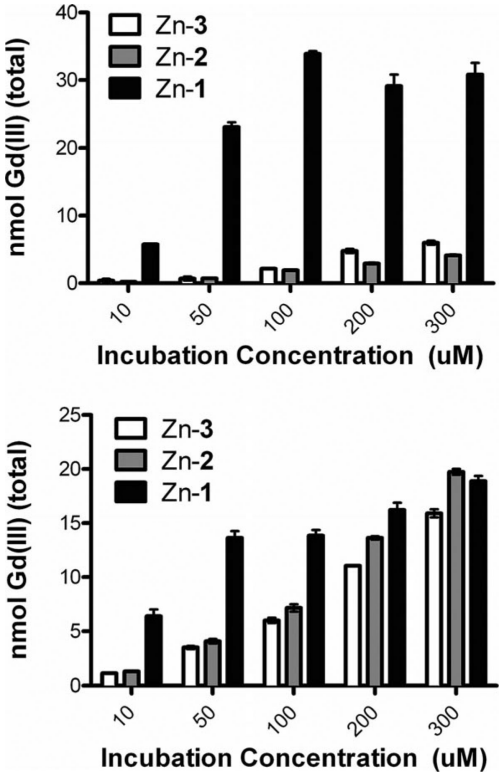

Figure 5.

In vitro cellular labeling of *S. aureus* and *E. coli* with Zn-**1**, Zn-**2**, and Zn-**3**. *S. aureus* (top) or *E. coli* (bottom) were incubated with increasing concentrations of Zn-**1** (black bars), Zn-**2** (gray bars), or Zn-**3** (white bars) at room temperature in LB broth. Gd^{III} content was analyzed by ICP-MS and is represented as the total amount of Gd^{III} per sample. Data are represented as the means ±SEM.

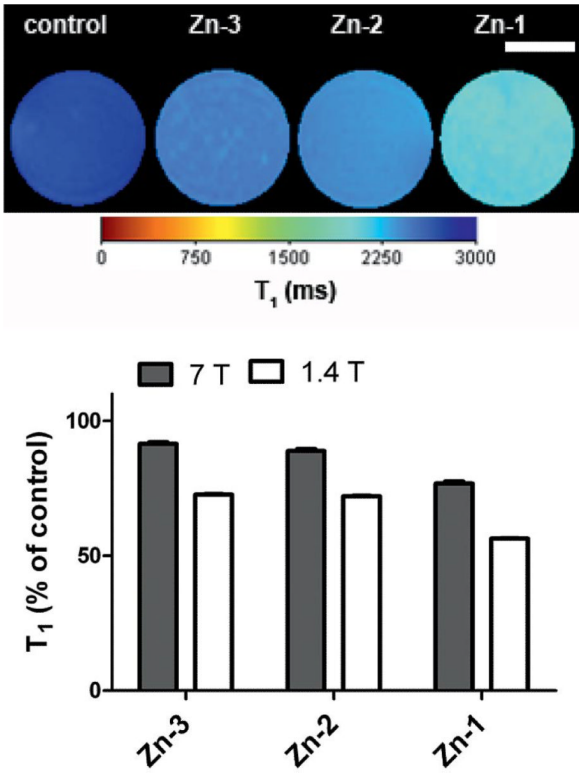

Figure 6.

S. aureus cultures were incubated with 300 μm Zn-**1**, Zn-**2** or Zn-**3**. Cells were washed 3 times with LB-broth and resuspended in 1% agarose. Scale bar represents 300 μm. Top: T_1-weighted map was acquired at 7 T at 25 °C (T_R/T_E = 500/11 ms). Cells labeled with Zn-1 are clearly brighter than both unlabeled bacteria and bacteria treated with Zn-2 or Zn-3. Bottom: T_1 relaxation times of agarose suspensions of *S. aureus* were measured using a saturation recovery pulse sequence with an echo time (T_E) of 11 ms and repetition times (T_R) as indicated in the Experimental Procedures at 7 T and 1.41 T. Data are presented as the percent reduction in T_1 vs. bacteria incubated with LB media, washed, and suspended in agarose.